

Chloride Diffusivity in Red Mud-Ordinary Portland Cement Concrete Determined by Migration Tests

Daniel Vêras Ribeiro^{a*}, João Antonio Labrincha^b, Márcio Raymundo Morelli^a

^aDepartment of Materials Engineering, Federal University of São Carlos, Rod. Washington Luis, Km 235, CEP 13565-905, São Carlos, SP, Brazil

^bDepartment of Ceramics and Glass Engineering, University of Aveiro & CICECO, Campus Universitário de Santiago, CEP 3810-193, Aveiro, Portugal

Received: January 8, 2011; Revised: April 15, 2011

Red mud, which is a solid waste produced in the alumina production process, is classified as dangerous due to its high pH. In this work, the concentration of chlorides was monitored by measuring the conductivity of the anolyte, which initially was distilled water. The steady and nonsteady-state chloride diffusion coefficients were estimated from the “time lag” and “equivalent time” between diffusion and migration experiments. The capillary water absorption, apparent porosity and pore size distribution of concretes were also analyzed. The addition of red mud apparently ensured lower chloride diffusion in the tested mixtures due to its superfine particle-size distribution and its “filler” effect. Red mud lengthened the service life of the concrete to 35 years (double that of the reference concrete). This finding is very positive since it indicates a delay in the onset of the rebar corrosion process caused by the migration of chloride ions.

Keywords: concrete, red mud, nondestructive testing, migration

1. Introduction

The huge volumes of industrial waste produced today represent one of the world's greatest environmental problems. With an annual volume of up to 25 million tons of waste generated in São Paulo alone, Brazil faces this industrial growth paradigm. The red mud of this study is a by-product of aluminum production from bauxite ore produced by the Bayer process. The Brazilian NBR 10004/2004 technical standard classifies red mud as dangerous, and the worldwide production of red mud exceeds 117 million tons/year. These vast quantities of wastes call for the search for widely consumed target products into which they can be incorporated, and motivated this study of the influence of added red mud on the characteristics of cement mortars and concrete.

Red mud is the main waste generated in the production of aluminium and alumina by the Bayer process from bauxite ore. Bauxite mines are located in three main climate regions: the Mediterranean, Tropical and Subtropical¹. The world's production of bauxite in 2009 was 205 million tons, and the main producing countries were Australia, China, Brazil, Guinea, India and Jamaica. Ranking third in worldwide production in 2009, Brazil produced 26.6 million tons of bauxite. It also has the world's third largest bauxite ore reserves (around 3.5 billion tons), concentrated mainly in the northern part of the country (State of Pará)².

Approximately 35-40% of bauxite ore is discarded in the form of strongly alkaline RM slurry³. This mud contains about 60 vol. (%) of solid content in the form of superfine particles. Therefore, this material has a large surface area, strong water absorbing capacity, and long-term persistence of alkalinity.

Alkaline matrices such as those provided by Portland cement in mortars and concrete are commonly used in waste conditioning. They are inexpensive, have an extensively documented history of safe use, and are a draw-upon readily-accessible technology. Alkalinity greatly reduces the solubility of many hazardous inorganic species and inhibits microbiological processes. Moreover, since these

matrices require water for hydration, they may readily incorporate wet wastes⁴ such as red mud. The search for an economically and environmentally viable alternative has led to the study of red mud for various applications, such as a component of clinker⁵⁻⁷, while its addition to mortar and concrete formulations was also reported⁸.

The behavior of concrete depends on its porous structure and pore size distribution⁹, and particularly on its durability and resistance to the penetration of aggressive agents such as chloride ions. The relative amount of capillary pores and the degree of interconnection play a crucial role in the transport of such substances through the concrete. It is widely known that chloride ions cause local breakdown of the passive layer and subsequent corrosion of reinforcing steel bars (rebars) in concrete structures.

The pores in concrete form a network connected to the outside, which enable the penetration of gas, water and aggressive dissolved substances into the concrete. The destruction of concrete and corrosion of rebars depend on this porous structure, which governs the degradation mechanisms.

Pore sizes in cement paste vary by several orders of magnitude. According to Siebeert apud Freire¹⁰, pores can be classified as trapped air pores (formed during the consolidation of concrete); air incorporated pores (obtained using air entraining additives), capillary pores (from free water in the concrete); and gel pores (due to water gel). The first three types of pores exert the greatest influence on the durability of concrete.

Pores larger than 0.1 microns (10^{-7} m) contribute to mass transport by diffusion, ion migration, capillarity and permeability, while smaller pores affect only the gaseous diffusion process and ion migration.

In recent years, migration tests have been widely used for accelerated testing of chloride diffusion in concrete, covering steady-state and non-steady-state migration regimes¹¹. Due to the complexity of the transport mechanisms involved, however, a

*e-mail: verasribeiro@hotmail.com

theoretical correlation between results obtained from distinct methods is still lacking. In the literature, experimental data for establishing this correlation are also very limited.

Capillary absorption is an important mechanism involving the penetration of chloride into concrete. In contact with a salt solution, unsaturated concrete will absorb this solution by capillary forces. The simultaneous action of diffusion and capillary suction thus causes a mixed transport mode, which is present in most of the conditions to which reinforced concrete structures are exposed¹².

The initial mechanism appears to be suction, especially when the surface is dry and salt water is rapidly absorbed by dry concrete. The capillary movement of salt water through the pores is then followed by a more substantial diffusion.

The water absorption of a concrete is difficult to control. In principle, smaller capillary pores exert greater capillary pressure, thus inducing greater and faster absorption. This phenomenon is demonstrated by Young's Equation 1:

$$\gamma_{SG} - \gamma_{SF} = \gamma_{FG} \cos\theta \quad (1)$$

where γ_{SF} is the solid-fluid surface tension, γ_{FG} is the fluid-gas surface tension, γ_{SG} is the solid-gas surface tension, and θ is the contact angle.

According to Helene¹³, lower water/cement ratios appear to help reduce absorption. However, because they increase the density and compactness of concrete, they also reduce the diameter of capillary pores, and if the pores are interconnected, capillary absorption may increase. At the other extreme, porous concrete absorbs small quantities of water by capillary forces, but other common problems such as permeability and carbonation may be more pronounced.

Diffusion is the process whereby substances are transported from one environment to another due to a difference in chemical potential, often concentration. Diffusion is a spontaneous process of mass transport, which is caused by effect of the concentration gradients of two different environments in close contact with each other, through which the substance diffuses to equalize the concentration.

This phenomenon occurs with both liquid and gaseous substances. Thus, the action of the two main aggressive agents in a reinforced concrete, chloride ions and CO_2 , is controlled by this phenomenon. Moreover, oxygen penetration, which is essential for the progression of the cathodic reaction, also occurs by diffusion⁹.

Diffusion flow occurs in two ways: (i) through *steady-state* diffusion, which is characterized by the constant flow of substances; (ii) and *nonsteady-state* diffusion, in which the flow is dependent on penetration time and depth. These states can be represented, respectively, by the Fick's first and second laws.

In the diffusion of chloride ions in concrete, *nonsteady-state* diffusion is the period when the transport of ions occurs in combination with its attachment to the cement phases, while *steady-state* diffusion is the period when the flow occurs at a constant rate (Castellote apud Santos⁹).

Several studies^{11,14,15} report the use of migration tests to evaluate the resistance of concrete to penetrating chloride ions. Initially, these tests were used to evaluate this penetration based on the total penetrated load, according to the ASTM C 1202/1992 standard, and to estimate the diffusion coefficient in *steady-state* conditions, as suggested by Andrade¹⁴. More recently, several authors have used migration tests to calculate the diffusion coefficient in *nonsteady-state* conditions^{11,15}. Depending on the proposed objective, these tests may vary in terms of procedure and parameters, but all are based on the induction of the movement of ions under the action of an external electric field⁹.

The migration test is based on the principle of applying a potential difference between two cells: one containing a chloride solution

(cathode) and the other without chlorides (anode), which are placed on each side of the concrete sample under analysis. The externally applied electric potential forces the passage of chloride ions through the concrete sample from the first (cathode) to the second (anode) cell.

By this method, the passage of chloride ions through the specimen is induced by the electric current generated by the potential difference of 12 volts applied to a direct current source through the electrodes contained in each cell. The positive cell (anode) is filled with distilled water to prevent corrosion-induced deposition of chlorides. The negative cell (cathode) is composed of a solution containing a concentration of 1 M of sodium chloride (NaCl).

2. Experimental

2.1. Materials

Ordinary CP-II 32 Z Portland cement (OPC), according to the Brazilian NBR 11578 standard, commercially available in São Carlos, Brazil, was selected as reference in all the tests.

The coarse aggregate was dense, crushed granitic stone and the sand was supplied from a river deposit commercially available in São Carlos, Brazil. The red mud came from Poços de Caldas-MG and was supplied by ALCOA Brazil. It is a mixture containing about 60% of solids, collected immediately after alumina recovery from the digestion process.

2.2. Methods

The materials characterization involved X-ray diffraction (Rigaku Geigeflex ME 210GF2 Diffractometer) and X-ray fluorescence (Philips PW1480 X-ray Fluorescence Spectrometer) analyses, while physical parameters such as the specific surface area (estimated by BET, using a Micrometrics Gemini 2370 V1.02 equipment) and specific gravity (Helium Pycnometer Accupyc 1330 V2.01 from Micrometrics) were also determined. Similar determinations were performed on sand and on the red mud.

The mortar formulation used as reference was prepared in a 1.0 : 1.5 : 1.3 : 0.5 (Portland cement + red mud : sand : coarse aggregate : water) weight ratio. Distinct concrete mixtures in which cement was partially replaced by red mud (10, 20, and 30% in weight) were analyzed.

The mortar content was 65.8% and the cement consumption was 540 kg.m⁻³ compared to a reference mixture. After mixing, a vibrating table was used to ensure efficient compaction. Concentrations of 0.5, 1.0 and 1.5% (per cement mass) of a superplasticizer were used for 10, 20 and 30% of red mud contents, respectively. The reference mixture did not require the addition of plasticizer. This procedure ensured a similar workability for all the mixes (230 ± 10 mm). Table 1 describes the consumption of material per cubic meter (m³) of produced concrete and the characteristics of the mixtures.

All the specimens were cylindrical. To determine the apparent porosity and pore size distribution, and to perform the migration tests, specimens of 50 mm in diameter and 100 mm in length were molded, from which 40 mm thick slices were cut, discarding the outer top and bottom parts in order to minimize heterogeneities and ensure water saturation.

Capillary water absorption was determined from cylindrical specimens 200 mm in length and 100 mm diameter. The specimens were demolded 24 hours after being cast and were cured for 28 days in a humid chamber (>95% RH). Samples 15 × 15 × 30 mm were taken from these specimens to determine the pore size distribution. A minimum of 4 samples were tested in all determinations.

Table 1. Consumption of materials and characteristics of concrete mixtures (RM = red mud).

Mixture proportions (cement + RM : fine aggregate : coarse aggregate : water)				
	1.0 : 1.5 : 1.3 : 0.5			
Added red mud contents	0%	10%	20%	30%
Cement (kg.m ⁻³)	540.0	486.0	432.0	378.0
Superplasticizer (L.m ⁻³)	0.0	2.6	5.1	7.5
Red mud (kg.m ⁻³)	0.0	54.0	108.0	162.0
Water/binder ratio	0.5	0.5	0.5	0.5
Mortar content (%)	65.8	65.8	65.8	65.8
Workability – Slump (mm)	240.0	236.0	231.0	225.0

The apparent porosity was verified using a technique based on the Archimedes principle. The samples were weighed in the dry condition (M_s) and then immersed in water for 24 hours until they reached full saturation, after which the immersed mass (M_i) and the wet mass (M_w) were determined. Thus, the apparent porosity (P_A) was calculated according to Equation 2.

$$P_A(\%) = 100 \cdot \rho_L \cdot [(M_w - M_i)(M_w - M_i)] \quad (2)$$

The ρ_L is the liquid density (in this in case, water, $\rho_L = 1.0 \text{ g.cm}^{-3}$ at 25 °C). The pore size distribution was measured by mercury intrusion porosimetry (Micromeritics Poresizer 9320).

The American ASTM C-1202/97 standard (Standard Test Method for Electrical Indication of Concretes Ability to Resist Chloride Ion Penetration) advocates the use of vacuum saturated samples before submission to migration tests. This procedure has been adopted by other researchers^{9,15} to ensure that the penetration of chlorides into the sample was caused predominantly by diffusion. In this work, vacuum saturation was not used; instead, the samples were soaked in water for 24 hours prior to testing.

The selection of samples representative of each composition is a complex task due to the large diversity of components (and relative ratios). Therefore, an adaptation of the ASTM E 562-99 Standard Test Method for Determining Volume Fraction by Systematic Manual Point Count was used. According to this standard, the relative amount (%) of a certain target phase (gravel, in this work) can be estimated by superimposing a grid on the sample and then counting the intersecting nodes in the middle and edges of the target phase, as indicated in Figure 1. In this example, the grid contains 38 nodes, and intersections with gravel correspond to 15 points (12 in the middle + 6 (x 0.5) at the edges). Thus, 15/38 would yield an estimated 39.5 vol. (%) of gravel in the sample. From an initial total of eight samples per composition, the four samples having the most similar composition were selected and tested.

PVC cells were used, consisting of a 50 mm diameter “T” tube with a top cover for output measurements and a side containing the electrode, properly sealed to prevent loss of solution. The specimens were placed at the interface between the two chambers, and were also glued with a silicone-based adhesive. Thus, the ion exchange between cells took place only through the body surface-to-test exposed area. The test setup and its implementation are illustrated in Figures 2a and 2b, respectively. A 12-Volt current was applied to the system by means of electrodes positioned at the ends of the cell, which were connected to copper wires from a controlled voltage source.

The concentration of chlorides in the anolyte chamber (initially free of chlorides) was analyzed at regular intervals during the experiment using a portable digital conductivitymeter (CD-880,

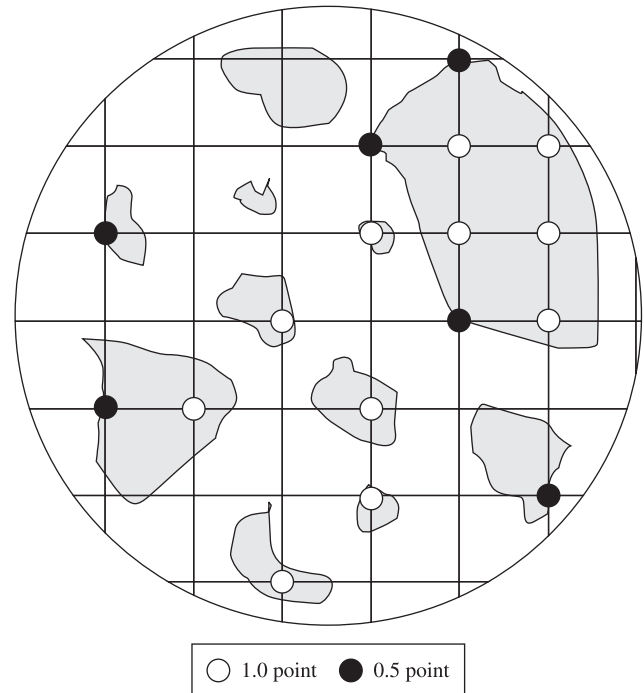


Figure 1. Process of sample selection and component quantification for chloride migration tests (in gray, the “gravel phase”); grid nodes inside the phase (in red) correspond to 1, while boundary intersection points (in black) correspond to 0.5.

Instrutemp). The chloride concentration was estimated based on the correlation between this parameter and the electrical conductivity, as indicated in Figure 3. Conductivity values were referenced to a temperature of 25 °C, by considering an increase of 2% in the conductivity of the solution when the temperature rose by one degree centigrade.

The capillary water absorption test was conducted according to the DIN 52617/87 standard, using cylindrical specimens 200 mm in length and 100 mm diameter. The sides of the specimens were sealed with silicon up to a height of 3 cm, leaving only one circular face of the specimen exposed to water. During the test, the water was kept at a constant level of 5 mm above the surface of the specimen in contact with water.

The specimen’s weight was monitored throughout the period it remained contact with water. Sorptivity, the volume of water penetrating per unit area and time, was calculated to facilitate the interpretation of the results. Sorptivity, S (kg/m².min^{0.5}), is determined empirically from the slope of the accumulated volume of water absorbed per unit area of inflow surface as a function of the square root of time, as indicated in Equation 3.

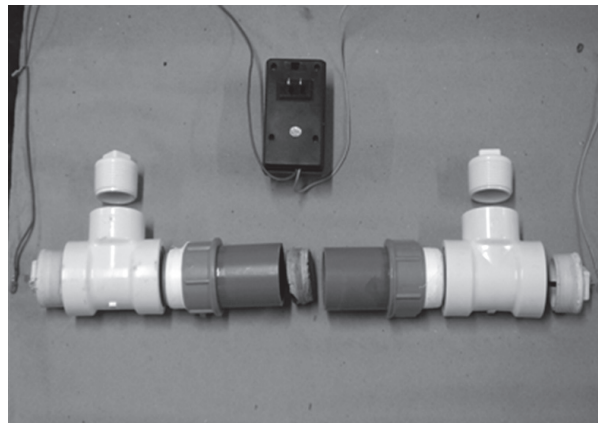
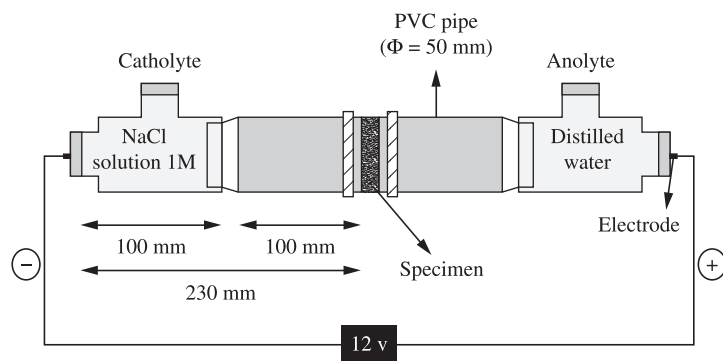
$$V_w / A_c = S \cdot \sqrt{t} + S_o \quad (3)$$

where V_w is the mass (or volume) of absorbed water (Kg), A_c is the cross-sectional area of each specimen (m²), and t is the time of exposure (minutes).

3. Results and Discussion

3.1. Materials characterization

The Portland cement used in this work has a specific surface area 0.93 m².g⁻¹ and its specific gravity is 3.11 kg.dm⁻³. The sand



(a)



(b)

Figure 2. a) Layout and assembly of the chloride migration test; and b) Chloride migration test apparatus.

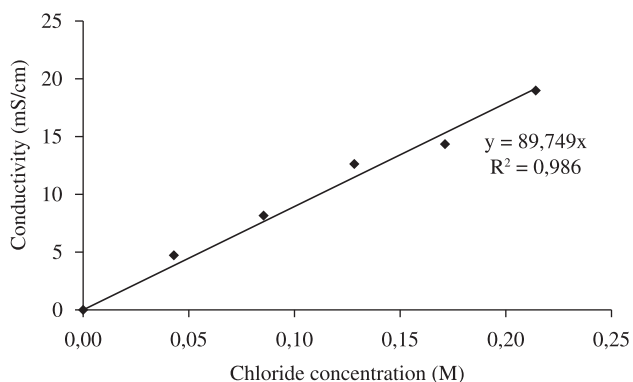


Figure 3. Experimental correlation between conductivity (at 25 °C) and chloride concentration in the anolyte chamber initially containing distilled water.

has a specific surface area of $0.68 \text{ m}^2 \cdot \text{g}^{-1}$ and its specific gravity is $2.70 \text{ kg} \cdot \text{dm}^{-3}$. According to Brazilian NBR 7211 standard, it is classified as fine sand. The gravel has a specific gravity of $2.74 \text{ kg} \cdot \text{dm}^{-3}$ and maximum dimension of 19 mm.

The red mud was received in the form of a paste containing about 40% free water. In the present study, the material was dried and

crushed, and then used as a powdered additive. Ideally, if its potential as a constituent of concrete is confirmed, red mud should be incorporated and tested in the as-received condition, and the free water present in the mud should be considered a component of the mortar mix.

The specific surface area of bauxite waste is $20.27 \text{ m}^2 \cdot \text{g}^{-1}$, as indicated by the particle fineness illustrated in Figure 4. Its maximum particle size is under $40 \mu\text{m}$ and the mean value is only about $8 \mu\text{m}$. The specific gravity is $2.90 \text{ kg} \cdot \text{dm}^{-3}$ and the pH is very high (12.95), exceeding the limit (12.5) for non-hazardous wastes established by the Brazilian NBR 10004 standard.

Table 2 gives the chemical composition of the waste, while Figure 5 shows the corresponding XRD pattern. As expected, aluminium hydroxide ($\text{Al}(\text{OH})_3$), calcium carbonate (CaCO_3), and iron oxide (Fe_2O_3) are the predominant components, but the relative amounts of SiO_2 and Na_2O (or NaOH) are also relevant. Some of these oxides were also detected by XRD, in addition to aluminium hydroxide and a complex $\text{Na}_5\text{Al}_3\text{CSi}_3\text{O}_{15}$ phase.

3.2. Effects on properties

3.2.1. Apparent porosity and pore size distribution

Figure 6 illustrates the evolution of apparent porosity of the cured concrete at different ages as a function of the relative amount of added

Table 2. Chemical composition of red mud estimated by XRF.

Component	Al ₂ O ₃	Fe ₂ O ₃	Na ₂ O	CaO	SiO ₂	K ₂ O	MnO	TiO ₂	Others	LOI *
Content (wt. (%))	19.87	19.85	7.35	4.61	14.34	1.87	0.21	2.66	1.01	27.20

* LOI = Loss on ignition.

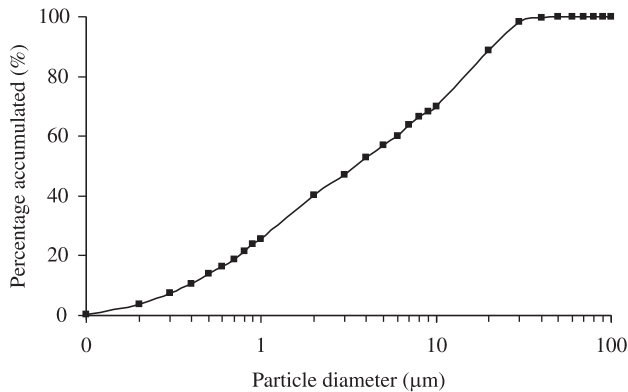


Figure 4. Particle size distribution of the dry red mud.

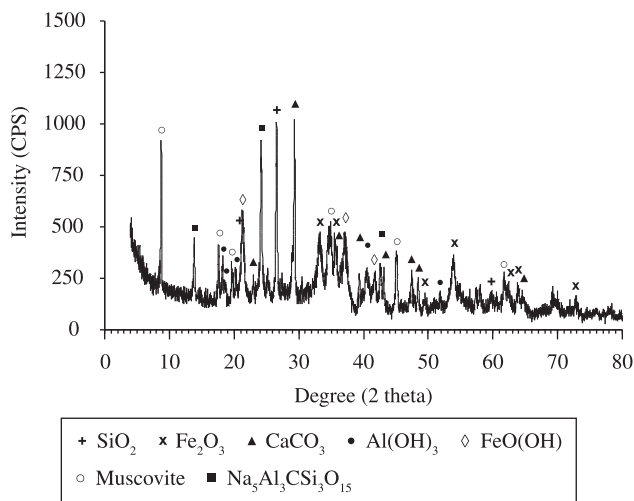


Figure 5. X-ray diffraction (XRD) pattern of dry red mud.

mud. The figure clear indicates that the overall variation is small (less than 5% in absolute terms). Due to the extreme fineness of bauxite waste, the compactness of concrete is expected to increase along with increasing contents of red mud, up to certain limit (particle packing theory), thereby reducing its porosity. However, this tendency has not been proved. The samples' pore size distribution was determined to help our interpretation of the results (Figure 7).

Keeping in mind that capillary pores have “diameters” of 0.01 to 1 µm, Figure 7 clearly shows that the pores of concrete samples without red mud (0%) are concentrated precisely in the median portion of this range (about 0.1 µm). In response to the addition of red mud, the pore size distribution becomes less homogeneous and larger voids or macropores (close to 1 µm in diameter) are generated, leading to an increase in total porosity, as clearly indicated in Figure 7.

This unexpected tendency reveals mixing and compaction difficulties during the preparation of waste-containing mixtures.

3.2.2. Chloride migration test

Figure 8 shows the evolution of chloride concentration in the anolyte chamber during migration tests. As expected, Cl⁻

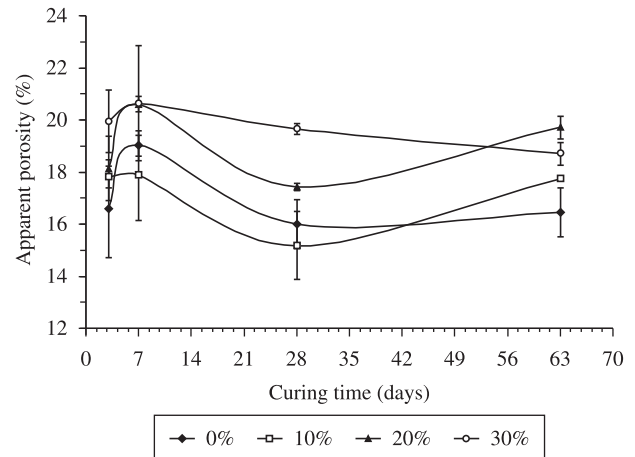


Figure 6. Apparent porosity of concrete containing red mud as a function of curing time.

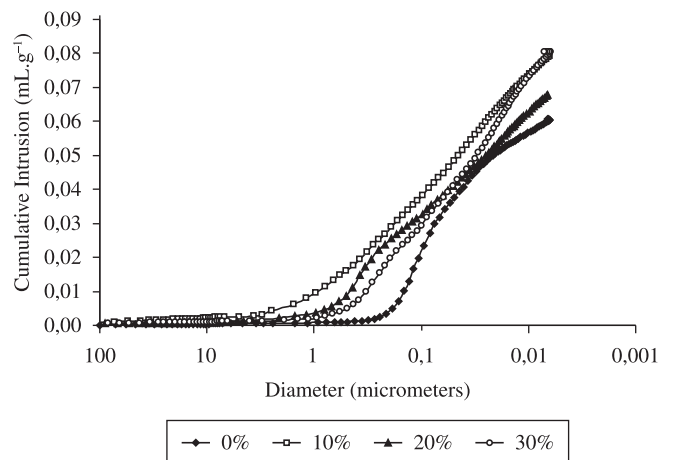


Figure 7. Change in the cumulative porosity of concrete with different red mud contents (0-30%) after 28 days of curing.

concentration increases with time once the voltage is applied, following the predictable trend.

Initially, there is a period in which the amount of chlorides passing into the anolyte chamber is negligible. Its duration corresponds to the so-called “time lag” (τ), and can be defined as the time required for chlorides to pass through the concrete disc, causing its saturation. This period of time will later serve as the basis for estimating the D_{ns} values. After this period, the flux of chloride ions through the specimen becomes constant, which corresponds to the steady-state period.

The “time lag” is empirically obtained from the intersection between the extension of the line that characterizes the steady-state and the time axis, according to the diagram of Figure 9.

Figure 10 shows that the time lag increases with increasing waste content, probably due to the reduction of a relative number of capillary pores. Moreover, the mud particles may close or interrupt

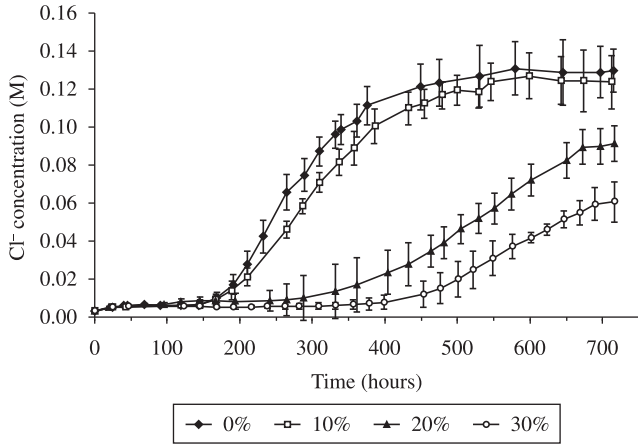


Figure 8. Evolution of Cl⁻ concentration in the anolyte chamber of a migration test cell over time, based on samples of concrete containing different amounts of red mud (0-30%).

the connectivity between some of those pores, thus diminishing the capillary suction of the concrete and hindering the transport of substances¹⁶. This occurs even in samples showing higher total porosity, meaning that within certain limits this parameter is not relevant. Microstructural changes should therefore be accounted for to better explain behavioral differences between the samples.

After the time lag, the flux of chloride ions through the specimen increases at a constant rate, which corresponds to the steady-state regime¹⁵. The steady-state diffusion coefficient (D_s) in migration tests is estimated using the Modified Nernst–Planck equation:

$$D_s = (J_{Cl}RTl) / (zFC_{Cl}\gamma\Delta\Phi) \tag{4}$$

where: J_{Cl} = flux of chloride ions (mol/cm².s); R = gas constant (1.9872 cal/mol.K); T = temperature (K); l = sample thickness (4 cm); z = ion valence (chlorides = 1); F = Faraday’s constant (23063 cal/volt.eq); C_{Cl} = chlorides concentration in the catholyte (mol.cm⁻³); γ = activity coefficient of the catholyte solution (Cl⁻ = 0.657) and $\Delta\Phi$ = effective applied voltage (12 V).

The chloride ion flux (J_{Cl}) represents the speed at which the ions are transported through the concrete, and the *steady-state* and *nonsteady-state* diffusion coefficients are calculated based on this flux. These coefficients can be calculated using the linear slope of the graph representing the evolution of the chloride concentration in the anodic cell as a function of time (Figure 9):

$$J_{Cl} = (V / A) \cdot (dC / dt) \tag{5}$$

where, A = exposed area (cm²); V = volume of the cathodic chamber (cm³).

The steady-state diffusion coefficient (D_{ns}) was calculated as follows. First, by estimating the enhancement or progress ratio obtained by applying an electrical field, comparing the time that chlorides would require under natural conditions of diffusion to reach the penetration depth observed in migration tests (t_{dif}), according to Equations 6 and 7.

$$1 / t_{dif} = (6 / \tau v^2) \cdot [v \cdot \coth(v / 2) - 2] \tag{6}$$

$$v = (ze\Delta\Phi) / kT \tag{7}$$

where: τ = *time-lag* in the migration test; t_{dif} = time equivalent if no electrical field were applied (s); e = 1.6 10⁻¹⁹ C; k = Boltzmann’s constant (1.38 10⁻²³ J.K⁻¹).

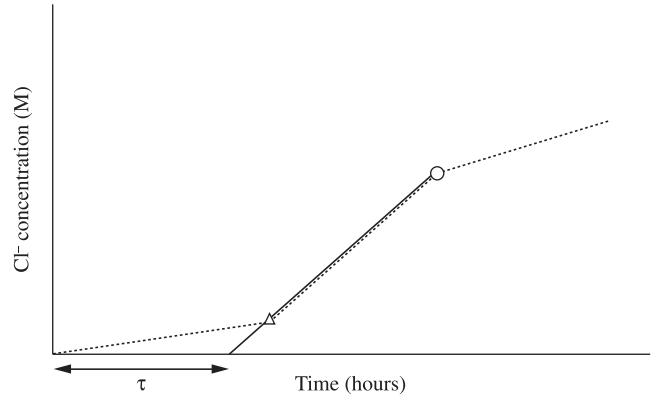


Figure 9. Experimental determination of the time lag (τ); onset (Δ) and end (O) of the steady-state diffusion stage, with a diffusion coefficient of D_s .

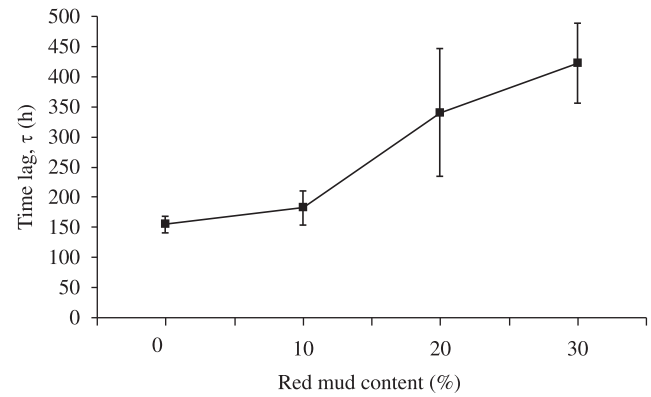


Figure 10. Time lag estimated from chloride migration tests as a function of red mud content in concrete cured for 28 days.

This mathematical solution allows migration tests to be “converted” into natural tests. In other words, using this “equivalent” time, t_{dif} , D_{ns} is obtained directly from Equation 8:

$$D_{ns} = l^2 / 3t_{dif} \tag{8}$$

where: l = specimen thickness (cm).

Figure 11 shows the flow of chloride ions, J_{Cl} , through the concrete as a function of red mud content in the material. This parameter represents the speed at which the ions are transported through the concrete and from which the steady-state and nonsteady-state diffusion coefficients (Figure 12) are calculated.

A clear decrease is observed in samples containing increasing amounts of waste. This is very positive because it reveals a delay in the onset of the corrosion process caused by the migration of chloride ions. These observations are in agreement with findings reported by Santos⁹ and Aitcin¹⁷, who showed the tendency of supplementary cementitious materials (such as red mud) to significantly reduce the mobility of chloride ions, reflecting the effect of increased tortuosity and better pore diameter distribution resulting from the pozzolanic reactions, which hinder ionic movement.

Moreover, red mud contains mineralogical phases such as sodium aluminosilicates, known as sodalites, i.e., zeolite-type compounds with an extremely high ion-exchange capacity, which makes red mud a good absorber of heavy metals¹⁸ and influences their surface properties¹⁹, including the formation of compounds by reaction with chloride ions. Other authors²⁰ also cite the importance of the presence of aluminates, which play an important role in anchoring

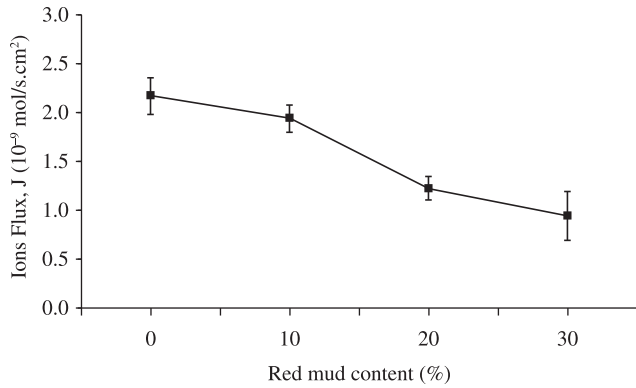


Figure 11. Chloride ion flow as a function of red mud content in concrete cured for 28 days, estimated from migration tests.

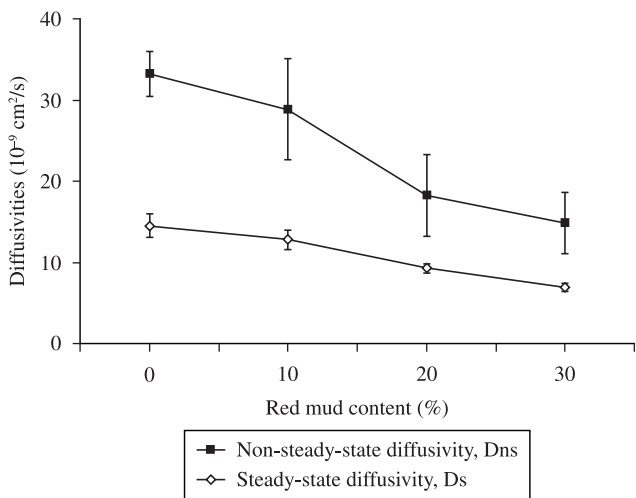


Figure 12. Steady-state and nonsteady-state diffusion coefficients of chloride ions as a function of red mud content in concretes cured for 28 days, estimated from migration tests.

the chloride ions, which would otherwise be free and available to start the corrosion process.

The aspects discussed in the above paragraph are also reflected in the steady-state and nonsteady-state diffusion coefficients of chloride ions shown in Figure 12, both of which decreased due to the addition of a higher red mud content.

Some authors^{9,15,21} attribute reductions of the diffusion coefficient to reductions in the water/binder (in this case, cement + red mud). However, they report a decrease in total porosity as this ratio diminishes, which was not the case in the present study. Therefore, our results cannot be correlated with a decrease in the water/binder ratio.

Figures 13 and 14 compare the depth of chloride penetration and the service life of concrete in order to more clearly illustrate the benefits of using red mud as a corrosion inhibitor in reinforced concrete¹². The results depicted in Figure 13 were obtained using Fick's second law of diffusion (Equations 9 and 10):

$$CP = 2(z)\sqrt{D_s t} \tag{9}$$

$$erf(z) = 1 - (C_{cl} - C_o) / (C_s - C_o) \tag{10}$$

where D_s is the steady-state diffusion (cm²/year), t is the service life (years), $erf(z)$ is the Gaussian error function, CP (chloride penetration) is

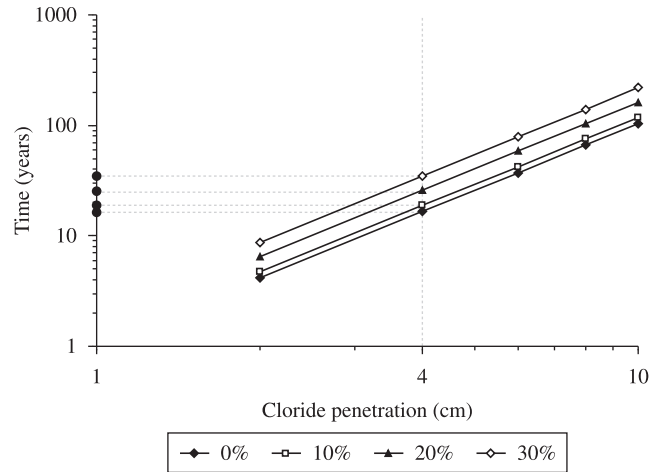


Figure 13. Correlation between time and depth of chloride penetration in concrete containing different amounts of red mud (to reach 0.4% Cl⁻ per weight of cement).

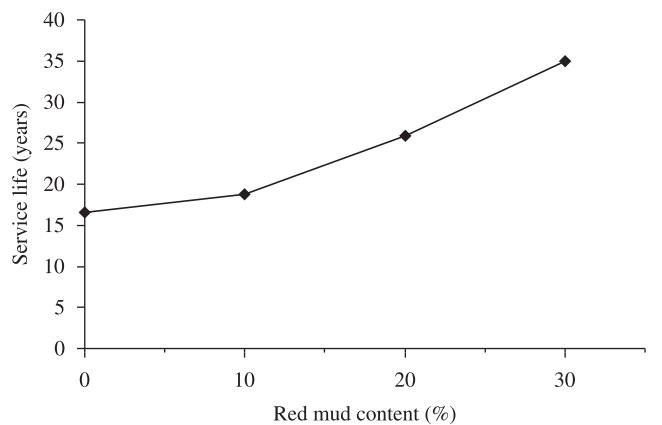


Figure 14. Correlation between estimated service life and red mud content in concrete, estimated from a chloride penetration depth of 4 cm depth in the structure.

the depth at which the chloride reaches the threshold limit concentration for rebar depassivation (cm), C_o is the initial chloride concentration (in this case, 0%), C_s is the chloride concentration at the surface (%), and C_{cl} is the chloride concentration as a function of depth and time (%).

Additionally, in line with the literature^{12,22}, several parameters were fixed: $C_s = 1.8\%$ and $C_{cl} = C_{dep} = 0.4\%$ per weight of cement, where C_{dep} is the chloride threshold limit concentration to depassivate the rebars (per weight of cement). The concrete layer is 4 cm thick and the formulation without red mud shows a service life of 16.5 years. As can be seen, the addition of red mud extends the service life of the concrete to up to 35 years (twice the service life of the reference concrete).

3.2.3. Capillary water absorption

Figure 15 shows the sorptivity values of concretes containing different amounts of red mud estimated from capillary water absorption tests. As mentioned earlier, finer red mud particles tend to diminish the relative amount of capillary pores. Therefore, the capillary suction decreased from 0.078 kg/m².min^{0.5} (concrete without red mud) to 0.015 kg/m².min^{0.5} (30% red mud content).

It should be noted that diffusion and capillary water absorption are not the only factors responsible for the durability of structures. Other factors such as alkali-aggregate reaction and carbonation are relevant and are also under evaluation.

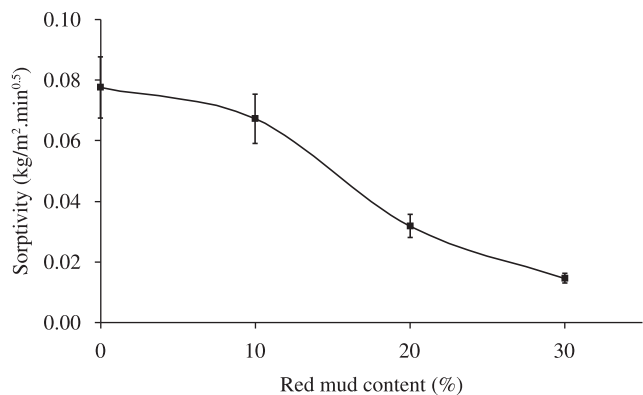


Figure 15. Water absorption of concrete specimens as a function of red mud content.

4. Conclusions

Chloride contamination in an exposed reinforced concrete structure is one of the most challenging forms of degradation to correct. The ingress of chloride ions in concrete occurs by chloride diffusion or penetration of contaminated water through capillarity. This research led to the following conclusions:

- For chloride migration testing, the use of distilled water as the initial anodic solution facilitates the measurement of the evolution of the chloride concentration based on the solution's conductivity, yielding excellent results in a simple way, at low cost and with high reproducibility;
- The presence of pores with a diameter of about 1 μm facilitates the ingress and diffusion of chloride ions in concrete through diffusion and capillary suction;
- The addition of red mud reduces the amount of capillary pores and/or promotes their blockage due to the high fineness of red mud particles. Nevertheless, the total porosity of the concrete remains unchanged and even increases slightly (about 5%);
- The direct consequence of reducing the steady-state diffusion coefficient is the extension of the service life of concrete structures;
- The time lag increases with increasing red mud content as a result of the reduction in the relative amount of capillary pores;
- The decrease in the interconnectivity between capillary pores in samples containing red mud and the presence of typical mineralogical phases such as sodium aluminosilicates, known as sodalites, are responsible for reducing the flow of chloride ions, and hence, the steady-state and nonsteady-state diffusion coefficients; and
- The chloride migration tests of samples of concrete containing red mud showed a longer service life, reaching more than double that of the reference samples (16.5 versus 35 years).

Acknowledgements

The authors wish to thank the *CNPq* - National Council of Technological and Scientific Development (Brazil), *PPGCEM/UFSCar* - The Postgraduate Program in Materials Science and Engineering at the Federal University of São Carlos (Brazil) and the *UA/DECV* - Ceramics and Glass Engineering Dept., University of Aveiro & *CICECO* (Portugal) - Project FCT-PTDC/CTM/65243/ 2006, for their support of this research. *This project did not have the financial support of Alcoa Brazil.

References

1. Brazilian Aluminum Association - ABAL. *O alumínio*: alumínio primário. São Paulo: ABAL; 2009. Available from: <www.abal.org.br/aluminio/producao/alupri.asp>. Access in: 13/05/2010.

2. Brazilian Mining Association - IBRAM. *Bauxita*. Brasília: IBRAM; 2009. Available from: <http://www.ibram.org.br/sites/1300/1382/00000033.pdf>. Access in: 15/05/2010.
3. Ekrem K. Utilization of red mud as a stabilization material for the preparation of clay liners. *Engineering Geology*. 2006; 87:220-229. doi:10.1016/j.enggeo.2006.07.002
4. Glasser FP. Fundamental aspects of cement solidification and stabilization. *Journal of Hazardous Materials*. 1997; 52:151-170. doi:10.1016/S0304-3894(96)01805-5
5. Singh M, Upadhayay SN and Prasad PM. Preparation of iron rich cements using red mud. *Cement and Concrete Research*. 1997; 27(7):1037-1046. doi:10.1016/S0008-8846(97)00101-4
6. Tsakiridis PE, Agatzini-Leonardou S and Oustadakis P. Red mud addition in the raw meal for the production of Portland cement clinker. *Journal of Hazardous Materials*. 2004; B116:103-110. PMID:15561368. doi:10.1016/j.jhazmat.2004.08.002
7. Singh M, Upadhayay SN and Prasad PM. Preparation of special cements from red mud. *Waste Management*. 1996; 16(8):665-670.
8. Cabeza M, Collazo A, Novoa XR and Pérez MC. Red mud as a corrosion inhibitor for reinforced concrete. *Journal of Corrosion Science Engineering*. 2003; 6:1-4. doi:10.1016/S0956-053X(97)00004-4
9. Santos L. *Avaliação da resistividade elétrica do concreto como parâmetro para a previsão da iniciação da corrosão induzida por cloretos em estruturas de concreto*. [Tese]. Brasília: Brasília University; 2006.
10. Freire KRR. *Avaliação do desempenho de inibidores de corrosão em armaduras de concreto*. [Tese] Brasília: Federal University of Paraná; 2005.
11. Tong L and Gjörv OE. Chloride diffusivity based on migration testing. *Cement and Concrete Research*. 2001; 31:973-982. doi:10.1016/S0008-8846(01)00525-7
12. Medeiros MHF and Helene P. Surface treatment of reinforced concrete in marine environment: Influence on chloride diffusion coefficient and capillary water absorption. *Construction and Building Materials*. 2009; 23:1476-1484. doi:10.1016/j.conbuildmat.2008.06.013
13. Helene PRL. *Corrosão em Armaduras para Concreto Armado*. São Paulo: PINI; 1999.
14. Andrade C. Calculation of diffusion coefficients in concrete from ionic migration measurements. *Cement and Concrete Research*. 1993; 23:724-742. doi:10.1016/0008-8846(93)90023-3
15. Castellote M, Andrade C and Alonso C. Measurement of the steady and nonsteady-state chloride diffusion coefficients in a migration test by means of monitoring the conductivity in the anolyte chamber comparison with natural diffusion tests. *Cement and Concrete Research*. 2001; 31:1411-1420. doi:10.1016/S0008-8846(01)00562-2
16. Song G. Equivalent circuit model for SAC electrochemical impedance spectroscopy of concrete. *Cement and Concrete Research*. 2000; 30:1723-1730. doi:10.1016/S0008-8846(00)00400-2
17. Aitcin PC. The durability characteristics of High Performance Concrete: a review. *Cement and Concrete Composites*. 2003; 25:409-420. doi:10.1016/S0958-9465(02)00081-1
18. Chvedov D, Ostap S and Le T. Surface properties of red mud particles from potentiometric titration. *Colloids Surface A*. 2001; 182:131-141. doi:10.1016/S0927-7757(00)00814-1
19. Lopez E, Soto B and Arias M. Adsorbent properties of red mud and its use for wastewater treatment. *Water Research*. 1998; 32:1314-1322. doi:10.1016/S0043-1354(97)00326-6
20. Yadav VS, Prasad M, Khan J, Amritphale SS, Singh M and Raju CB. Sequestration of carbon dioxide (CO₂) using red mud. *Journal of Hazardous Materials*. 2010; 176:1044-1050. PMID:20036053. doi:10.1016/j.jhazmat.2009.11.146
21. Ampadu KO, Torii K and Kawamura M. Beneficial effect of fly ash on chloride diffusivity of hardened cement paste. *Cement and Concrete Research*. 1999; 29:585-590. doi:10.1016/S0008-8846(99)00047-2
22. Nilsson L, Andersen A, Luping T and Utgenannt P. Chloride ingress data from field exposure in a Swedish road environment. In: *Proceedings of the Second International Rilem Workshop on Testing and Modelling the Chloride Ingress into Concrete*; 2000; Paris. Paris: RILEM Publications SARL; 2000.